JOURNAL OF VIROLOGY, Nov. 2005, p. 14330–14338 Vol. 79, No. 22
0022-538X/05/$08.00+0 doi:10.1128/JVI.79.22.14330–14338.2005

Rational Attenuation of a Morbillivirus by Modulating the Activity of the RNA-Dependent RNA Polymerase

David D. Brown,[1] Bertus K. Rima,[1] Ingrid V. Allen,[1] Michael D. Baron,[2] Ashley C. Banyard,[2] Thomas Barrett,[2] and W. Paul Duprex[1]*

School of Biomedical Sciences, The Queen's University of Belfast, 97 Lisburn Road, Belfast BT9 7BL, United Kingdom,[1] *Institute for Animal Health, Pirbright Laboratories, Ash Road, Pirbright, Woking GU24 0NF, United Kingdom*[2]

Received 29 June 2005/Accepted 8 August 2005

Negative-strand RNA viruses encode a single RNA-dependent RNA polymerase (RdRp) which transcribes and replicates the genome. The open reading frame encoding the RdRp from a virulent wild-type strain of rinderpest virus (RPV) was inserted into an expression plasmid. Sequences encoding enhanced green fluorescent protein (EGFP) were inserted into a variable hinge of the RdRp. The resulting polymerase was autofluorescent, and its activity in the replication/transcription of a synthetic minigenome was reduced. We investigated the potential of using this approach to rationally attenuate a virus by inserting the DNA sequences encoding the modified RdRp into a full-length anti-genome plasmid from which a virulent virus (rRPV^{KO}) can be rescued. A recombinant virus, rRPV^{KO}L-RR$_{EGFP}$R, which grew at an indistinguishable rate and to an identical titer as rRPV^{KO} in vitro, was rescued. Fluorescently tagged polymerase was visible in large cytoplasmic inclusions and beneath the cell membrane. Subcutaneous injection of 10^4 TCID$_{50}$ of the rRPV^{KO} parental recombinant virus into cattle leads to severe disease symptoms (leukopenia/diarrhea and pyrexia) and death by 9 days postinfection. Animals infected with rRPV^{KO}L-RR$_{EGFP}$R exhibited transient leukopenia and mild pyrexia, and the only noticeable clinical signs were moderate reddening of one eye and a slight ocular-nasal discharge. Viruses that expressed the modified polymerase were isolated from peripheral blood lymphocytes and eye swabs. This demonstrates that a virulent morbillivirus can be attenuated in a single step solely by modulating RdRp activity and that there is not necessarily a correlation between virus growth in vitro and in vivo.

Morbilliviruses cause significant levels of disease in humans and animals throughout the world. For example, the human pathogen measles virus (MV) infects over 40 million individuals per annum and leads to the death of around 800,000 children. The classical course of disease progression is difficult to mimic comprehensively in tractable animal models as the virus has a highly restricted host range. A number of nonhuman primate models have been developed which reproduce many, but not all, aspects of the human disease. However, each has some limitations and they are all dead-end hosts (2, 45, 47). This limitation has led to the development of a range of small-animal models, which are useful but tend to reflect only limited aspects of the human disease (29, 30, 33, 37, 40). These models are augmented by others which use closely related morbilliviruses, such as rinderpest virus (RPV) or canine distemper virus (CDV), to infect natural hosts such as cattle and ferrets (18, 49, 52). Although many aspects of MV infection of humans are mirrored in the pathogenesis of CDV and RPV, each has its characteristic pattern of disease progression. Thus, wild-type CDV is much more likely to infect the central nervous system than MV, whereas RPV has not been found to infect the central nervous system. In contrast, wild-type RPV has a particular propensity to infect the intestinal epithelium compared to what is observed in MV or CDV infections. Nevertheless, these other diseases can be used to study aspects of MV pathogenesis, and infection leads to the generation of symptoms consistent with those commonly associated with MV, such as pyrexia, profound leukopenia, and associated immunosuppression and viremia. Five distinct phases have been described for a wild-type RPV infection: after a short incubation period of between 3 and 5 days, the body temperature rises rapidly, severe mouth lesions and nasal and ocular mucopurulent discharges are observed, extreme dehydration and weakness follow, and the animal either dies or recovers (8). Recovery may take several weeks. During the infection the virus replicates extensively in lymphocytes, macrophages, and epithelial cells of, among other systems, the gastrointestinal tract.

Morbilliviruses have genomes of between 15,690 and 15,948 (3) nucleotides comprised of negative-strand RNA tightly encapsidated into a ribonucleoprotein (RNP) complex (22). The viruses have six transcription units that encode at least two nonstructural and six structural proteins. Three of these, the nucleocapsid (N), phospho- (P), and large (L) proteins along with the RNA, comprise the RNP. Complexes of the two transmembrane glycoproteins, the hemagglutinin (H) and fusion (F) proteins, bind cellular receptors and mediate virus-to-cell fusion. The hydrophobic matrix (M) protein associates with both the cytoplasmic tails of F and H and the RNP.

The L protein contains the majority, if not all, of the catalytic functions associated with the RNA-dependent RNA polymerase (RdRp). It is essential that every virion contains a functional RdRp. Following entry, it acts as a transcriptase that sequentially generates capped, polyadenylated mRNAs from

* Corresponding author. Mailing address: School of Biomedical Sciences, The Queen's University of Belfast, Belfast BT9 7BL, Northern Ireland, United Kingdom. Phone: 44 28 9097 2060. Fax: 44 28 9097 5877. E-mail: p.duprex@qub.ac.uk.

each transcription unit during primary transcription. The transcriptase probably enters the genome either at a single promoter in the 3′ end of the genome or at the beginning of the N gene. It potentially transcribes the leader region, although this short RNA has not been detected in infected cells (11). After transcribing a gene, it encounters a gene-end signal and then the intergenic trinucleotide. At this point it can either detach from the RNP or continue to transcribe the next gene, beginning at the gene-start signal. This progressive start-stop mechanism leads to a transcription gradient whereupon the transcripts from the promoter distal L gene are present in much lower amounts.

In previous work we have demonstrated that it was possible to introduce the open reading frame of enhanced green fluorescent protein (EGFP) within the L gene of MV (14). This was guided by an alignment of the morbillivirus L proteins (28), which indicated that there are three highly conserved domains (D1, D2, and D3) separated by two variable "hinges" (H1 and H2). The modified polymerase was 40% less efficient in standard minigenome assays, and even though the resulting virus, EdtagL-MM^{EGFP}M, replicated to similar titers as the unmodified virus, there was a lag of approximately 5 h as determined by growth analysis. At that time we proposed that this approach could provide a means to rationally attenuate virus replication. However, this could not be tested as EdtagL-MM^{EGFP}M is based on a vaccine strain of MV, and no wild-type MV natural host model is available. This constraint can be overcome as a rescue system, which permits the generation of a virulent virus, has been developed for the RPV Kabete "O" (RPV^{KO}) wild-type strain (4, 5). This, alongside the availability of a well-characterized animal model for RPV infection, offers the opportunity to demonstrate that insertion of EGFP into an RdRp is not restricted to MV, to determine if other recombinant viruses can be recovered, and to test our hypothesis that it may be possible to attenuate a morbillivirus in a single step by modifying the RdRp.

MATERIALS AND METHODS

Cell culture and viruses. HeLa cells were grown as described previously (15). B95a cells (26), were grown in RPMI medium 1640 (Invitrogen) supplemented with 5% (vol/vol) fetal calf serum (FCS; Invitrogen). The recombinant wild-type Kabete "O" strain (rRPV^{KO}) was rescued and passaged in B95a cells (5). Vaccinia viruses, vTF7-3 and MVA-T7, were grown in primary chicken embryo fibroblasts as previously described (6, 15).

Animals. Six-month-old out-bred Friesian Holstein bullocks were used in all animal experimentation. The cattle were obtained from the Institute for Animal Health, Compton, and were housed in the Specific Animal Pathogens Order category 4 animal isolation units at the Institute for Animal Health, Pirbright. Animals were fed on commercial pelleted food concentrates and hay. All infection protocols were carried out under an approved Home Office license for animal experimentation.

Growth analysis. B95a cells were cultured to 95% confluence in plastic dishes with a diameter of 35 mm. Cells were infected at a multiplicity of infection (MOI) of 0.5 for 2 h at 37°C, after which time the inoculum was removed. Cells were incubated at 37°C and infections were terminated at regular intervals, up to 72 h, by freezing to −70°C. Supernatants were clarified by centrifugation 1,500 rpm for 5 min at 4°C. Virus titers were determined by infection of B95a cells in triplicate 50% endpoint dilution assays (41) and are expressed in 50% tissue culture infective doses/ml ($TCID_{50}$/ml).

Construction of pEMC-L(RRR)^{KO}. An analogous approach to that used for MV was taken to generate a plasmid which expresses the wild-type Kabete 'O' RdRp using the insertion vector pEMCassette (14). The plasmid was assembled in four steps by PCR amplification of RPV^{KO} sequences from pT7KOL.4 (5) using oligonucleotides containing a range of restriction sites (underlined). Domain 1 of RPV^{KO} was amplified using oligonucleotides priRPV^{KO}9236+ (5′-TAT TTC ACC ATG GAC TCC CTC TC-3′) and priRPV^{KO}11080BssHII− (5′-TCT AGA CGC GCG CGA GAT ACC AGC C-3′). Upon treatment with NcoI and BssHII, this fragment could be ligated into similarly treated pEMCassette to generate pEMC-L(R)^{KO}. Due to the presence of an AatII restriction site in the RPV^{KO} L gene open reding frame (ORF), domain 2 was amplified in two fragments (D2a and D2b). Domain 2b of RPV^{KO} was amplified from the endogenous AatII site to the H2 region using primers priRPV^{KO}12858BssHII+ (5′-AAC TGT CAG CGC GCT GAC ATA GAT AGA GAG ACG *AGC* GCA CTC AGG GTC CCC TAC-3′), which contained a BssHII restriction site, a BsmBI restriction site, and three nucleotide changes (italics) to silently ablate the endogenous AatII restriction site, and priRPV^{KO}14328AatII− (5′-CAG CGG CGA CGT CAT GCT GAA AGT TG-3′). Following digestion with BssHII and AatII, this fragment could be ligated into similarly treated pEMC-L(R)^{KO} to generate pEMC-L(RRb)^{KO}. Domain 2a was amplified using oligonucleotides priRPV^{KO}11115BssHII+ (5′-GTA TCT CGC GCG CGT CTA GAA ATG A-3′) and priRPV^{KO}12817− (5′-CTG AGT GCT GAC GTC TCT CTA TCT ATG TCA-3′). Upon digestion with BssHII and BsmBI, this fragment could be ligated into similarly treated pEMC-L(RRb)^{KO} to generate pEMC-L(RR)^{KO}. Domain 3 was amplified using oligonucleotides priRPV^{KO}14356AatII+ (5′-TTC AGC ATG ACG TCG CCG CTG ATA TGC-3′) and priRPV^{KO}15734Eco47III− (5′-CGA ATG AGA GCG CTG TAA CCT ATT AG-3′). Following treatment with AatII and Eco47III, this fragment could be ligated into similarly treated pEMC-L(RR)^{KO} to generate pEMC-L(RRR)^{KO}, which contained all three domains of RPV^{KO} L (indicated by an R) and unique restriction sites in the sequences encoding H1 and H2. DNA sequencing was carried out to confirm that no spurious mutations were present in the cDNA clone.

Insertion of EGFP in hinge 2 of RPV polymerase. The complete EGFP ORF, in which the stop codon has been mutated to a glycine codon, was obtained from pEMC-La(MM^{EGFP}M) by restriction digestion using AatII (14). This fragment was ligated into AatII-restricted pEMC-L(RRR)^{KO} to generate pEMC-L(RR^{EGFP}R)^{KO}. Restriction digestion and DNA sequencing were used to confirm that the EGFP ORF was present in the correct orientation.

Assessment of polymerase function. The ability of the pGEM-L (6), pEMC-L(RRR)^{KO}, and pEMC-L(RR^{EGFP}R)^{KO} plasmids to express functional polymerase proteins was determined using a standard minigenome replication/transcription assay using a negative-sensed mini-genome plasmid, p(−)RPVDICAT (L. J. Rennick et al., unpublished data). MVA-T7-infected HeLa cells grown to a confluence of 60% were transfected as previously described (14) using pKSN1, pKSP (6), the appropriate L expression plasmid, and p(−)RPVDICAT.

Generation of EGFP-tagged recombinant RPV. The multiple cloning site of pGEM5Zf(+) was modified to include an NarI site (10). A subclone, pscRPV^{KO}(NarI), was generated from a full-length cDNA clone of RPV^{KO} (pRPV^{KO}) (5) in this modified vector. The subclone was restricted with NcoI and BstEII to remove a fragment containing the region encoding H2 within the L gene. This was replaced with the corresponding region from pEMC-L (RR^{EGFP}R)^{KO} to generate pscRPV^{KO}R^{EGFP}R(NarI). The plasmid was digested with NarI and the 5,322-bp fragment, now containing the EGFP ORF, was introduced into the full-length plasmid pRPV^{KO} to generate pRPVKO-L(RR^{EGFP}R). Rescue of the recombinant virus was carried out in B95a cells, grown to a confluence of 65% in 35-mm-diameter wells, infected with vTF7-3 at an MOI of 0.5. Transfections were carried out using Transfast reagent (Promega). Liposome complexes, made using plasmids RPV^{RK} N (1 μg), RPV^{RK} P (1 μg), RPV^{RK} L (50 ng), pRPV^{KO}-L(RR^{EGFP}R) (1 μg), and TransFast (3 μl/μg) were added to the cells for 1 h. Dulbecco's modified Eagle's medium containing 5% (vol/vol) FCS (1.5 ml) was added to each well, and the cells were incubated at 37°C with 5%(vol/vol) CO_2 for 3 days. After this time the medium was replaced with Dulbecco's modified Eagle's medium containing 2% (vol/vol) FCS (2 ml/well), and cells were examined daily for cytopathic effect. Recovery of virus was verified by the appearance of syncytia, and the recombinant viruses were cloned by limiting dilution twice on B95a cells.

RNA preparation and RT-PCR. Total RNA was prepared from rRPV^{KO}L-RR^{EGFP}R-infected B95a cells, peripheral blood mononuclear cells (PBMCs), and eye swabs using Trizol (Invitrogen). RNA was precipitated with isopropanol, and salts were removed by using cold 75% (vol/vol) ethanol. Two micrograms of total RNA was used as the template for cDNA synthesis using murine Moloney leukemia virus reverse transcriptase (RT) and random hexanucleotide primers. Controls in which RT was omitted were used to ensure amplification was not due to contaminating plasmid DNA. A universal P primer pair (5-ATG TTT ATG ATC ACA GCG GT-3′ and 5′-ATT GGG TTG CAC CAC TTG TC-3′), which produces an amplicon of 429 bp, or a virus-specific (5′-CTA TCC CTC GCT GGC-3′) and EGFP (5′-GGC ACG GGC AGC TTG CCG-3′) pair, which produces an amplicon of 350 bp, was used to detect virus RNA, and β-actin

primers (20) which produce an amplicon of 275 bp were used to verify the integrity of the total RNA.

Indirect immunofluorescence, autofluorescence, and confocal scanning laser microscopy. B95a cells were grown on glass coverslips in 35-mm-diameter petri dishes to a confluence of 90%. Cells were infected, fixed, and processed as previously described (16). The primary anti-RPV-H monoclonal antibody (C1) was used at a dilution of 1:40 (1). The Alexa Fluor 568-conjugated secondary antibody (Molecular Probes) was used at a dilution of 1:200. Coverslips were mounted in a single drop of Vectashield mounting medium (Vectorlabs) containing 4′,6 diamidino-2-phenylindole (DAPI). A Leica TCS SP2 Acousto-Optical Beam Splitter confocal scanning laser microscope (CSLM), equipped with UV and HeNe lasers as the source for the ion bean, was used to examine the samples for fluorescence and EGFP autofluorescence as previously described (16).

Animal infections, assessment of clinical signs, and sample collection. Animals were observed for 7 days prior to infection, and rectal temperatures were monitored daily. Viruses were diluted in RPMI medium (Invitrogen), and animals were infected by subcutaneous injection in the shoulder region with 10^4 $TCID_{50}$ of virus in a total volume of 1 ml. Animals were monitored daily for clinical signs of disease, and rectal temperatures were recorded. Blood samples were collected by jugular venipuncture using heparinized vacuum blood collection tubes (BD Vacutainer). Eye swabs were taken from both eyes using cotton buds. Animals were euthanized at the end of the experimental protocol and a complete postmortem was performed. Tissue samples were collected in formalin, embedded in paraffin, and processed, and 8-μm sections were cut using a microtome. Sections were stained using hematoxylin and eosin (HE) at the Histology Unit (Institute for Animal Health, Compton). Based on our extensive experience establishing this animal model, the resulting data, and ethical considerations, it was considered valid to assess virus attenuation using two animals. The reproducibility of the model makes us confident that data from historical controls could be used in a comparative pathological assessment.

Isolation of PBMCs. Whole blood (10 μl) diluted in 1% (vol/vol) glacial acetic acid (190 μl) was used to obtain a white blood cell count. Nonlysed cells were counted using an Improved Neubauer Hemocytometer. PBMCs were isolated from heparin-treated whole blood (20 ml) using Histopaque 1077 (Sigma-Aldrich) gradient centrifugation as previously described (23), and the final cell pellets were resuspended in phosphate-buffered saline (2 ml).

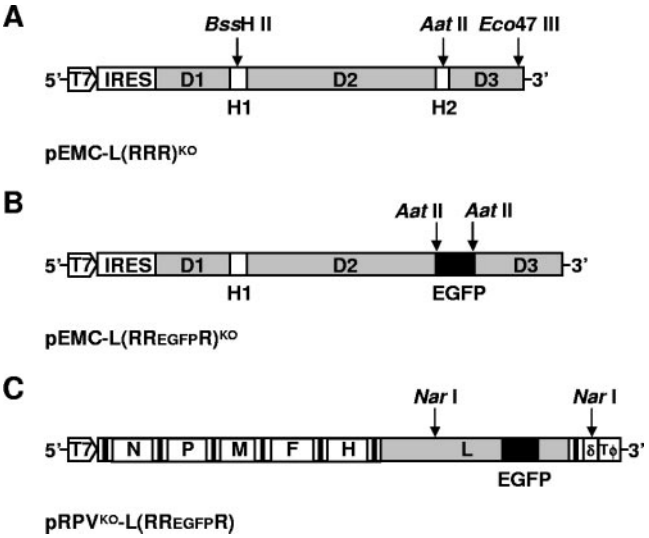

FIG. 1. Schematic representations of RPV^{KO} RdRp expression constructs and the full-length plasmid used to rescue the recombinant virus $rRPV^{KO}$L-RREGFPR. The positions of the T7 promoter, internal ribosome entry site (IRES), three domains of the RdRp (D1 to D3), hinge regions of the RdRp (H1 and H2), hepatitis delta ribozyme (δ), and T7 terminator (Tφ) are indicated (not to scale). The RdRp ORF is shown in gray and the EGFP ORF is black. (A) Unmodified RPV^{KO} RdRp expression construct. (B) Expression construct engineered to include the EGFP ORF within the H2 region of the RPV^{KO} RdRp. (C) Structure of $pRPV^{KO}$L-RREGFPR encoding an antisense genome copy of RPV^{KO} in which the EGFP ORF was inserted into H2 of the RdRp. Untranslated regions flanking ORFs are represented as open boxes, and solid lines indicate the positions of the intergenic trinucleotide spacers.

RESULTS

In vitro assessment of the functionality of an RdRp derived from a virulent rinderpest virus containing EGFP within the protein. The RBOK vaccine strain (RPV^{RK}) was derived from the wild-type virulent RPV^{KO} strain (38). These viruses are different by 0.55% at the nucleotide level, and there are 33 amino acid differences between the strains (7). The RPV^{KO} L protein is 2,183 amino acids in length. An expression plasmid was constructed for the RPV^{KO} L, and this included a number of unique restriction sites (Fig. 1A). Introduction of the BssHII site resulted in a single amino acid alteration (L627V→A), whereas introduction of the AatII site resulted in two amino acid changes (L1708E→D and L1709Q→V). Introducing the Eco47III site did not lead to amino acid changes in the protein. However, this site is located 15 nucleotides from the end of the L ORF, and as pEMCassette was designed for the expression of a MV polymerase, this leads to two additional amino acid differences (L2182R→K and L2183E→D).

To date, the insertion of 238 amino acids within an RdRp with concomitant retention of function has only been demonstrated for MV. In order to extend this finding, equivalent sequences encoding EGFP were inserted into the AatII site in pEMC-L$(RRR)^{KO}$ to generate plasmid pEMC-L$(RR_{EGFP}R)^{KO}$ (Fig. 1B). The modified polymerase proteins were used to rescue an RPV minigenome plasmid containing a chloramphenicol acetyltransferase (CAT) reporter gene in order to assess their relative functionality over a range of concentrations. In a negative control experiment, plasmid encoding L was omitted. This confirmed that CAT activity was solely due to RdRp-mediated replication/transcription (data not shown). Both L gene expression plasmids were diluted to give a range of 1 μg to 100 pg, and transfections were carried out in triplicate (Fig. 2). The plasmids encoded functional polymerases and expression from pEMC-L$(RRR)^{KO}$ yielded comparable levels of CAT activity in this assay to those obtained using a plasmid (pGEM-L) that expresses an authentic RPV^{RK} polymerase (31,171 ± 82.3 cpm using 10 ng of plasmid and 54,950 ± 674.3 cpm using 400 ng of plasmid). Maximum levels of CAT activity were obtained when 10 ng of polymerase-expressing plasmid was used in the transfection. Interestingly, the relative level of CAT activity obtained in cells expressing the EGFP-containing polymerase compared to the unmodified polymerase varied significantly over the six experiments. Thus, relative activities ranged from 85%, when 1 ng was transfected, to 1%, when 1 μg was transfected, of the unmodified control. This observation indicates the importance of transfecting a range of plasmid amounts when performing minigenome assay experiments designed to examine relative polymerase efficiencies. These results demonstrate that the ability to tolerate a large insertion of 11% within the polymerase is not unique to MV.

Generation and molecular characterization of $rRPV^{KO}$L-$RR_{EGFP}R$. The efficient, albeit diminished, rescue of the virus minigenome by the RPV polymerase containing EGFP indicated that it might be possible to generate a recombinant virus

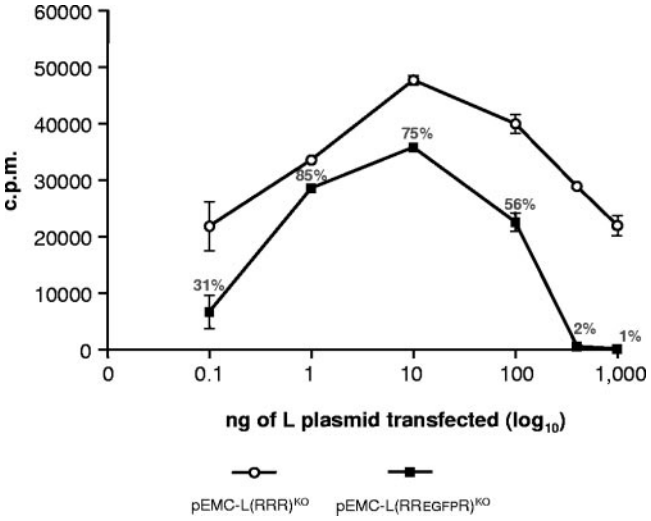

FIG. 2. Relative activities of unmodified and EGFP-modified polymerase in a series of minigenome rescue experiments. Various amounts of pEMV-L(RRR)^{KO} (open circles) and pEMV-L(RR^{EGFP}R)^{KO} (filled circles) were used in minigenome transfection assays. The amount of acetylated ^{14}C-chloramphenicol produced was determined by liquid scintillation counting and is expressed in counts per minute (c.p.m.). Percentage figures represent the relative activity of the structurally modified RdRp compared to the unmodified control.

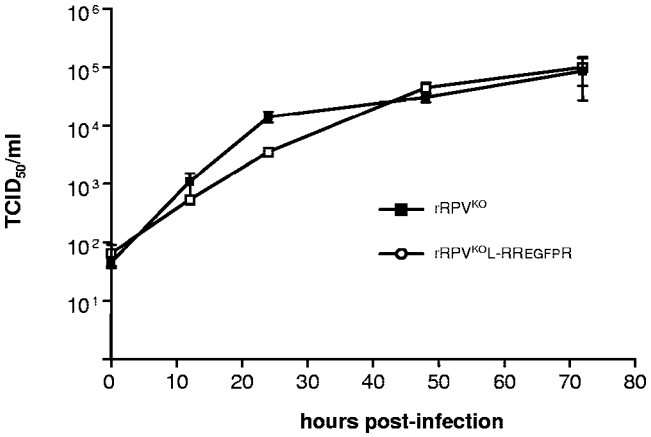

FIG. 3. Growth kinetics of recombinant RPVs. B95a cells were infected at an MOI of 0.5 with rRPV^{KO} and rRPV^{KO}L-RR^{EGFP}R. Titers were determined in triplicate and are expressed as $TCID_{50}$/ml. Lines join the average titers obtained, and error bars reflect the variability of the $TCID_{50}$ assay.

expressing this protein. To this end a full-length anti-genomic construct, pRPV^{KO}L-RR^{EGFP}R, which contained sequences encoding the modified polymerase, was generated (Fig. 1C). Recombinant virus rRPV^{KO}L-RR^{EGFP}R was recovered between 3 and 4 days posttransfection in four independent rescue experiments in B95a cells using the unmodified RPV^{RK} L-expression construct as a support plasmid. Nonfluorescent syncytia were never observed in the primary transfections, indicating that poxvirus-mediated recombination did not lead to loss of the EGFP sequences. An equivalent extent of cell-to-cell fusion to that seen in RPV^{KO} infected B95a cells was observed, and numerous secondary syncytia containing up to 50 nuclei developed in each infected monolayer. It is well established that pathogenicity of a morbillivirus can be diminished or even lost when the viruses are passaged on inappropriate cell lines (17, 25, 38). Animal studies have demonstrated that virulence is retained when RPV^{KO} is passaged on B95a cells; therefore, rRPV^{KO}L-RR^{EGFP}R was cloned by limiting dilution and was passaged five times in these cells to increase the titer. The growth characteristics of RPV^{KO} and rRPV^{KO}L-RR^{EGFP}R were examined by harvesting total virus at 0, 12, 24, 48, and 72 h postinfection (hpi) Titers were determined by a $TCID_{50}$ assay (Fig. 3). There was no difference in the overall rate of replication, and identical titers of approximately 10^5 $TCID_{50}$/ml were obtained by 72 hpi.

B95a cells were infected at an MOI of 0.5 with passage five rRPV^{KO}L-RR^{EGFP}R, total RNA was extracted from the cells at 72 hpi, and cDNA was synthesized. A 350-bp product which included the H2 encoding region and the 5′ region of the EGFP ORF was amplified by RT-PCR using RPV and EGFP-specific primers. Sequencing of the amplicon confirmed that the AatII restriction site and the EGFP ORF had been maintained during the five passages (data not shown).

Examination of the intracellular localization of the fluorescently tagged polymerase. B95a cells were infected at an MOI of 0.1 with passage five rRPV^{KO}L-RR^{EGFP}R. Fluorescence was readily detected by UV microscopy as early as 8 hpi. Both intracytoplasmic inclusions and membrane-associated EGFP autofluorescence were observed in unfixed living cells (data not shown). Fluorescence was detectable in all syncytia, indicating the stability of the recombinant virus during passage in vitro. In order to obtain a better indication of the intracellular localization of the EGFP-tagged polymerase cells, cells were grown on coverslips and infected at an MOI of 0.01. Cells were fixed 24 hpi and stained for H glycoprotein by indirect immunofluorescence. Nuclei were counterstained with DAPI, and samples were visualized by CSLM. Numerous intracytoplasmic inclusions were detected within syncytia, indicating that the sites of virus replication and the larger factories were in close association with the nuclear membrane (Fig. 4A). By this time point much of the H glycoprotein had trafficked to the cell membrane; RdRp was also detected around the periphery of syncytia. This was readily observed in single cells at higher magnifications, and most, if not all, of the cell membrane was decorated with H on the outside of the membrane and with EGFP-tagged RdRp on the inside (Fig. 4B and inset frame).

Pathogenicity of the recombinant rRPV^{KO}L-RR^{EGFP}R virus in cattle. The pathogenicity of rRPV^{KO}L-RR^{EGFP}R was compared to rRPV^{KO} in the natural host (5). Prior to infection both viruses were cloned by limiting dilution and passaged five times in B95a cells. Two 6-month-old out-bred Friesian Holstein bullocks (animals 1 and 2) were inoculated subcutaneously with 10^4 $TCID_{50}$ of rRPV^{KO}L-RR^{EGFP}R. Animals were monitored daily for typical signs of RPV infection. At 7 days postinfection (dpi) both animals exhibited reddening in one eye, and an ocular discharge was observed 8 and 9 dpi. No other clinical signs were observed and the animals were euthanized at 9 dpi. Control animals infected with rRPV^{KO} displayed significant clinical signs of RPV infection, including oral lesions, salivation, ocular and nasal discharges, leukopenia, pyrexia and diarrhea. Animals were euthanised at 9 dpi.

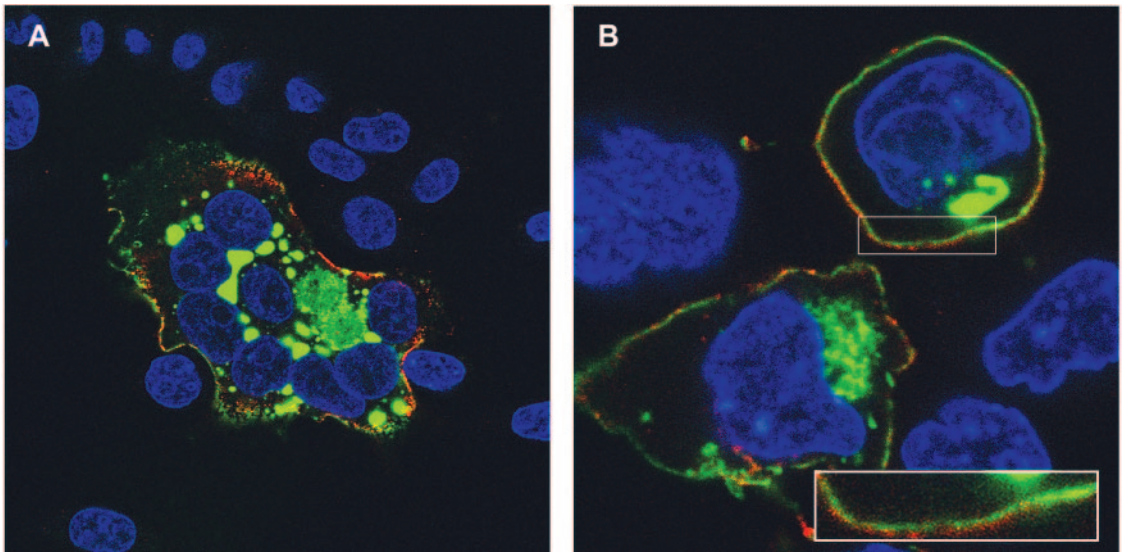

FIG. 4. Localization of EGFP-tagged RPV^{KO} polymerase and the H glycoprotein using CSLM. B95a cells were infected at an MOI of 0.01 with rRPV^{KO}L-RR$_{EGFP}$R for 24 h. RPV H was detected on the surface of nonpermeabilized cells using a mouse monoclonal antibody and visualized by indirect immunofluorescence using an Alexa Fluor 568–conjugated secondary antibody (red). EGFP was visualized by virtue of its autofluorescence (green). Nuclei were counterstained with DAPI (blue). (A) Photomicrograph of a syncytium comprised of eight infected cells. Magnification, ×1,432. (B) Composite photomicrograph of singly infected cells. Magnification, ×1,841. The inset is a magnification of a small region of the cell membrane indicated by the box.

Rectal temperatures fluctuated by no more than 1°C around the normal body temperature of 38.5°C prior to infection. After infection with rRPV^{KO}L-RR$_{EGFP}$R both animals exhibited elevations in temperature commencing either 4 or 5 dpi. Temperatures continued to rise to 40°C and 40.5°C at 7 dpi, after which time they returned to normal levels (Fig. 5A). Control animals infected with rRPV^{KO} displayed a more rapid and acute rise in temperature, which only decreased slightly when the animals became moribund (Fig. 5B).

Preinfection leukocyte levels varied between 8,500 and 9,500 cells/mm^3. Leukopenia was deemed to be severe if the total number of leukocytes/ml dropped to less than 50% of the preinfection level. All infected animals exhibited a loss of white blood cells shortly after infection. Leukopenia was less pronounced in rRPV^{KO}L-RR$_{EGFP}$R-infected animals, falling to just over 50% of the preinfection level, and also transient, as levels began to rise 7 dpi (Fig. 5A). In contrast in the rRPV^{KO} control animals levels dropped to ~25% of preinfection levels; numbers remained at this low level until animals were euthanized (Fig. 5B).

These data demonstrate that the rRPV^{KO}L-RR$_{EGFP}$R virus is attenuated for growth in cattle due to the presence of the EGFP within the RdRp. Both animals were euthanized at this time point in order to obtain time-matched samples for comparative pathological assessment and histopathology with tissues from rRPV^{KO}-infected animals. Samples of mesenteric lymph nodes, prescapular lymph nodes, eyelid, optic nerve, liver, spleen, abomasum, gall bladder, kidney, and small intestine were examined. Inflammation of the initial portion of the duodenum (animal 1) and the abomasum (animal 2) were the only indications that animals were infected.

Virus isolation, immunofluorescence, and RT-PCR confirms that the EGFP sequences are retained during replication in vivo. In the absence of overt clinical signs, attempts were made to isolate virus from PBMCs and eye swabs. Isolated PBMCs were cocultivated with B95a cells, and virus was recovered from both animals at 2, 4, 7, 8, and 9 dpi. Cell-to-cell fusion was evident in the B95a cells, and UV microscopy confirmed that the EGFP was detectable in all syncytia (Fig. 6A). These data were confirmed by RT-PCR amplification of viral sequences obtained from isolated PBMCs and eye swabs using morbillivirus universal P gene primers and control β-actin primers. Viral RNA was detected in the PBMCs at 7, 8 and 9 dpi (animal 1) and at 4, 7, 8, and 9 dpi (animal 2) (Fig. 6B) and in the eye swabs taken at 7 dpi (animal 1) and at 4 and 7 dpi (animal 2) (Fig. 6C). RT-PCR amplification using primers which amplify a region encoding the carboxyl terminus of D2 and the amino terminus of EGFP confirmed that the EGFP sequences were stably retained within the RdRp gene (data not shown).

Histological assessment. Extensive inflammation and ulceration of the gastrointestinal tract are a hallmark of wild-type RPV infection (52). The most significant levels of infection are found in the mesenteric lymph nodes and gut-associated lymphoid tissues, which become enlarged, soft, and edematous. HE staining was carried out on tissue samples from the animals infected with rRPV^{KO}L-RR$_{EGFP}$R and compared to tissue samples taken from a control animal infected with rRPV^{KO}. An area of mucosal inflammation which could be due to rRPV^{KO}L-RR$_{EGFP}$R infection was identified in the small intestine from animal 2 (Fig. 7A and inset frame). No significant perturbations of the gut epithelium were observed. Animals infected with rRPV^{KO} exhibited extensive ulceration of the small intestine epithelium (Fig. 7B). Prescapular lymph nodes isolated from the rRPV^{KO}L-RR$_{EGFP}$R-infected animals appeared normal (Fig. 7C), which is consistent with the rising

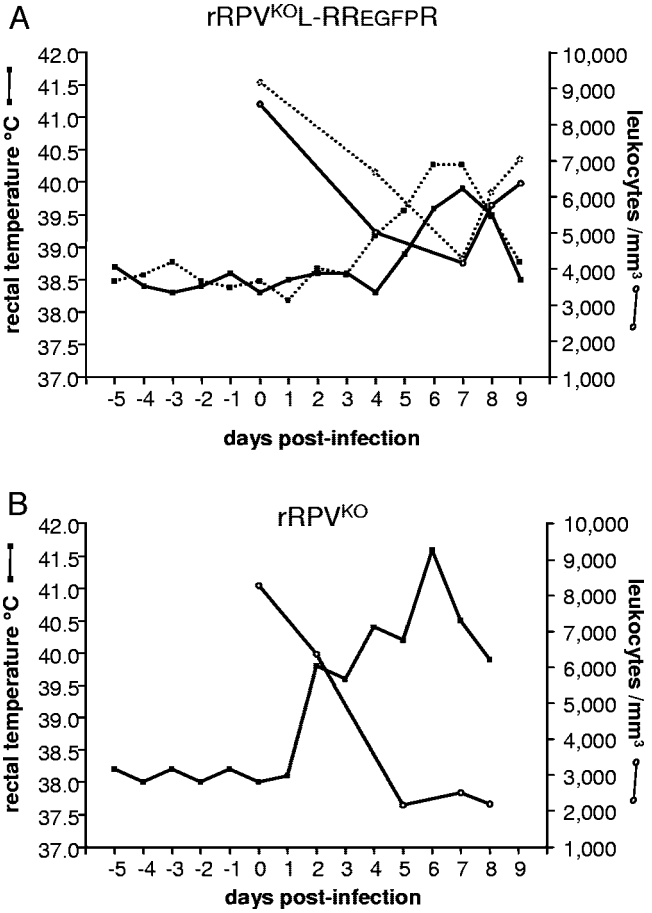

FIG. 5. In vivo assessment of virulence of recombinant RPVs. Cattle were infected with 10^4 $TCID_{50}$ with $rRPV^{KO}$ and $rRPV^{KO}$L-RR_{EGFP}R. Rectal temperatures were measured daily 5 days preinfection and daily up to euthanasia. White cell counts were determined at 2- to 3-day intervals postinfection. (A) Two animals (animal 1, solid line; animal 2, dashed line) were infected with $rRPV^{KO}$L-RR_{EGFP}R. The animals were euthanized at 9 dpi. (B) These data for $rRPV^{KO}$ represent control data which have been previously published (5) and have also been used as controls for an additional set of chimeric viruses (4).

leukocyte numbers. A significant reduction in total cell numbers in an equivalent region of the lymph node from the $rRPV^{KO}$-infected control animal was observed (Fig. 7D). This was the case for mesenteric lymph nodes and tonsils (data not shown). These data confirm that insertion of EGFP into the ORF of the RdRp leads to the single-step attenuation of rinderpest virus.

DISCUSSION

Many strategies have been used to attenuate viruses. Historically, vaccines were produced by repeated passage of clinical isolates in inappropriate host cells and at nonphysiological temperatures. Thus, the clinical MV isolate obtained from David Edmonston was passaged in chick embryos and chicken embryo fibroblasts to produce the Edmonston B virus (17, 25), which was shown to be attenuated in monkeys. This strain, as the Schwartz and other vaccine derivations, was administered to ~77% of the global target population in 2003, as estimated by the World Health Organization. Surprisingly, to this day, the underlying molecular basis of MV attenuation remains unknown. However, reverse genetics has allowed us to address this question for RPV, and the attenuation is due to alterations in multiple genes and promoter regions (4, 5). Cell culture adaptation strategies have yielded cold-adapted human respiratory syncytial virus (hRSV) (21) which has been further modified by chemical mutagenesis (13). The availability of reverse genetics systems provides an opportunity to rationally modify viruses, with the aim of generating new vaccines (51). Many of the hRSV-attenuating mutations map to the L gene, and those identified in cold-adapted hRSV mutants have been transferred into full-length clones to generate viruses with equivalent phenotypic properties (12, 24). These mutations and others identified in human parainfluenza virus 3 (44) have also been used to generate human parainfluenza virus 1 and 2 recombinants, which are attenuated in a hamster model (31, 34). Rearrangement of the gene order in studies using vesicular stomatitis virus and Newcastle disease virus also exemplifies the utility of reverse genetics-based approaches and viruses which reduced virulence in the natural host and in a small-animal model (19, 27). Complete genes have been deleted, for example, human and bovine RSV G gene (42, 46), and duplicated, for example, the F and G genes of human metapneumovirus (9). Such approaches are particularly attractive for members of the *Mononegavirales* as the viruses do not normally exhibit recombination. Thus, insertions, deletions, gene rearrangements, gene duplications, and/or the introduction of key site-directed attenuating mutations appear "locked" into the virus genome. We wished to exploit our studies which demonstrated that it is possible to add a complete EGFP within the polymerase of MV (14), first to determine if this is generally applicable to other morbilliviruses and, second, to establish if this approach could provide an opportunity to rationally attenuate a morbillivirus for which we have access to a natural animal host.

Minigenome assays provided the first indication that addition of EGFP led to a polymerase with lower activity and also suggested that this approach could have more widespread utility. Replication/transcription of the RNP was observed over a range of plasmid concentrations. In fact, measurable CAT activity was obtained using 10 pg of transfected pEMC-L $(RRR)^{KO}$ (data not shown) although in both cases optimal activity was obtained using 10 ng of the plasmid. To the best of our knowledge, we are not aware of such demonstrable polymerase activity over six logarithmic plasmid dilutions in a minigenome replication/transcription assay. These data demonstrate the importance of using a range of plasmid amounts when performing minigenome rescue experiments that aim to compare polymerase functionally. Thus, decreases in polymerase activity of either 15% or 99% could have been reported if we had used only single assays. The modified polymerase activity was less than that of the unmodified polymerase over all plasmid dilutions. This indicates that the defect in polymerase function cannot simply be overcome by expression of more protein. Conversely, when higher amounts of unmodified polymerases were expressed, CAT activity was decreased or virtually abolished in the case of the EGFP-tagged RdRp. Quantitative PCR has been used to propose a model of kinetics of RNA synthesis and to determine the processivity of both the

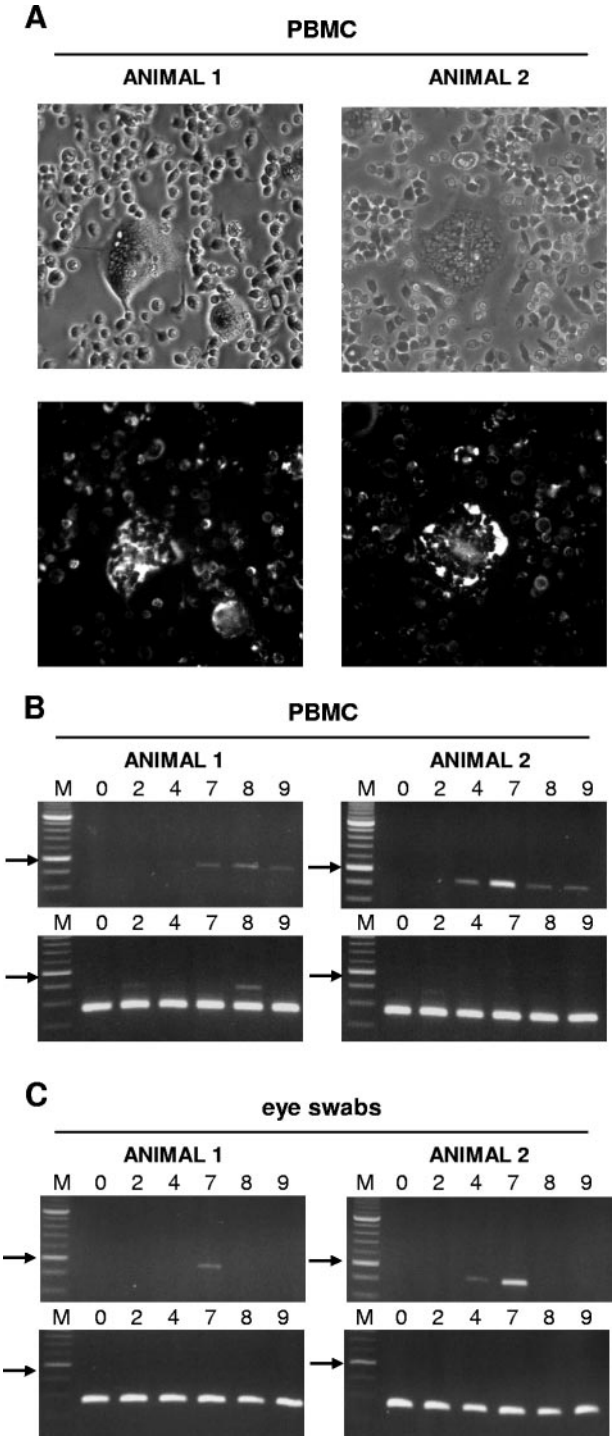

FIG. 6. Detection and virus isolation from clinical samples. (A) Phase-contrast and fluorescent photomicrographs of cytopathic effects due to rRPV^{KO}L-RR$_{EGFP}$R isolated from PBMCs of infected cattle. PBMCs were isolated from cattle infected for 4 days with rRPV^{KO}L-RR$_{EGFP}$R and overlaid onto B95a cells. Photomicrographs were taken 48 hpi using a digital CCQ camera (Hammatsu) attached to an Eclipse TE300 UV microscope (Nikon). Magnification, ×30. Total RNA was isolated from PBMCs and eye swabs obtained from rRPV^{KO}L-RR$_{EGFP}$R infected cattle 0, 2, 4, 7, 8 and 9 dpi. PCR products were amplified using morbillivirus universal P and β-actin primers from cDNA prepared from the total RNA. Amplicons were examined by DNA gel electrophoresis. Arrows indicate 500-bp DNA size markers. (B) Amplicons obtained from PBMC samples using the morbillivirus universal P primers (upper panels) and β-actin controls (lower panels). (C) Amplicons obtained from eye swab samples using the morbillivirus universal P primers (upper panels) and β-actin controls (lower panels).

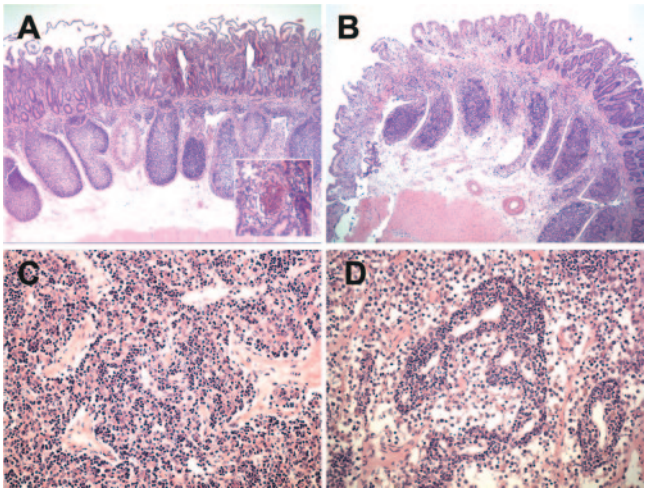

FIG. 7. Histological assessment of postmortem tissues obtained from animals infected with either rRPV^{KO}L-RR$_{EGFP}$R (sacrificed 9 dpi) or rRPV^{KO}. Sections were stained with HE, mounted, and viewed using a Leitz Dialux 22 microscope. Images were collected using a Leica DC 300 camera. (A) Small intestine including Peyer's patches showing reactive changes from animal 2 infected with rRPV^{KO}L-RR$_{EGFP}$R. The asterisk and inset frame indicate a focus of mucosal inflammation. Magnification, ×12. (B) Small intestine including Peyer's patches showing reactive changes from a control animal infected with rRPV^{KO}. Magnification, ×12. (C) Lymph node (prescapular) medullary region showing apparently normal cellularity from animal 1 infected with rRPV^{KO}L-RR$_{EGFP}$R. Magnification, ×75. (D) Lymph node (prescapular) medullary region showing a reduction in lymphocyte population from an animal infected with rRPV^{KO}. Magnification, ×75.

unmodified MV RdRp and the EGFP-tagged polymerase expressed by EdtagL-MM$_{EGFP}$M (39). In eukaryotic cells the unmodified polymerase elongates RNA at 3 nucleotides/second, whereas the structurally modified polymerase exhibits fivefold slower kinetics, elongating at 0.6 nucleotides/second. The ability to insert EGFP between two domains of the RdRp and retain function confirms the notion that the polymerase is a multidomain protein. We have recently made similar observations in our CDV rescue system (D. Silin et al., unpublished data).

Progression of rinderpest disease has been well described in both naturally and experimentally infected animals (32, 52). As rRPV^{KO}L-RR$_{EGFP}$R showed no growth impairment in vitro, we were interested to see if this was paralleled in animals and if virulence was retained. Our hypothesis that modulating the function of the RdRp by insertion of EGFP into the H2 region may reduce or completely abolish virulence was confirmed. It was clear that the virus replicated in vivo as pyrexia and leukopenia were observed, albeit at lower levels. Percentage decreases in PBMCs in rRPV^{KO}L-RR$_{EGFP}$R-infected animals was ~50%, which is equivalent to that observed in animals immunized with the rescued vaccine virus (rRPV^{RK}) alone or with recombinant versions of the vaccine which express either

influenza hemagglutinin-neuraminidase or soluble or membrane-bound forms of EGFP (50). This is also consistent with data obtained using a number of recombinant virulent CDVs in a small-animal system, which also provides a very sensitive readout of morbillivirus attenuation (48, 49). The RPV^{RK} vaccine is exclusively lymphotropic and, as such, is not shed from animals following vaccination. However, $rRPV^{KO}$L-RR^{EGFP}R was detected by RT-PCR from eye swabs. This and its ability to induce pyrexia indicate that $rRPV^{KO}$L-RR^{EGFP}R is less attenuated than $rRPV^{RK}$. However, there is a very significant reduction in pathogenicity, demonstrating that this approach could be a means of attenuating other viruses which at present lack an effective vaccine. Beyond these observations, a comparative pathological assessment was not made between the original RPV vaccine and $rRPV^{KO}$L-RR^{EGFP}R viruses in this study.

Systematic attenuation in a natural host has been reported for vesicular stomatitis virus by generating viruses with rearrangements in the gene order (19). Movement of the N gene from the promoter proximal position led to complete attenuation, with virus no longer being detected in the snout, nasal, and esophageal-pharyngeal fluids, suggesting that reduction in gene expression and associated replication are responsible for attenuation. Interestingly, these recombinant viruses all grew to equivalent titers as determined by $TCID_{50}$ even though they showed marked differences in virulence, illustrating the limitations of relating growth in tissue culture to pathogenesis. In order to address this, an analysis of relative virus fitness has been carried out for these viruses, and fitness values have been shown to correlate with the in vivo phenotypes (35; Gail Wertz, personal communication). This work therefore calls into question the merit of making extrapolations from in vitro growth data to in vivo natural infections and confirms our observations with $rRPV^{KO}$L-RR^{EGFP}R.

One of the advantages of these recombinant morbilliviruses is that they have allowed us a unique opportunity to sensitively detect an RdRp in infected cells (14). This is the first report which shows a clear association of a paramyxoviral polymerase with the inner leaflet of the cell membrane, and this may have implications for our understanding of the virus life cycle. This is very useful as there have been many technical difficulties associated with generating antisera which detect the polymerase. It is assumed that polymerases traffic from cytoplasmic inclusions to the cell membrane although the mechanism has not been elucidated. Our current data do not give any indication as to how the polymerase moves from these inclusions to the cell surface or if this is an actively facilitated or completely passive process. From these data there does not appear to be any particular targeting to specific regions of the cell membrane although some accumulation occurs where intracytoplasmic inclusions are in close proximity. Many positive stranded RNA viruses extensively modify and utilize membranes to facilitate their replication, and these have been suggested to represent topologically and functionally related structures (43). Although large intracytoplasmic inclusions are a feature of most paramyxovirus infections and these are generally considered to be the sites of virus replication, membrane rearrangements or vesiculation do not seem to be closely associated with these eosinophilic dense aggregates of viral nucleocapsid (36). We are currently extending these observations by using real-time confocal microscopy to examine the dynamics of the intracellular trafficking of both incoming and newly synthesized polymerases in order to better understand virus assembly and release.

ACKNOWLEDGMENTS

This work was supported by the Medical Research Council (grant 63468), the Wellcome Trust (grant 069411), and the BBSRC (grant BBS/B/00573).

We thank Paula Haddock for excellent technical assistance and Paul Monaghan for assistance with confocal scanning laser microscopy.

REFERENCES

1. **Anderson, J., and J. McKay.** 1994. The detection of antibodies against peste des petits ruminants virus in cattle, sheep and goats and the possible implications to rinderpest control programs. Epidemiol. Infect. **112:**225–231.
2. **Auwaerter, P. G., P. A. Rota, W. R. Elkins, R. J. Adams, T. DeLozier, Y. Shi, W. J. Bellini, B. R. Murphy, and D. E. Griffin.** 1999. Measles virus infection in rhesus macaques: altered immune responses and comparison of the virulence of six different virus strains. J. Infect. Dis. **180:**950–958.
3. **Bailey, D., A. Banyard, P. Dash, A. Ozkul, and T. Barrett.** 2005. Full genome sequence of peste des petits ruminants virus, a member of the *Morbillivirus* genus. Virus Res. **110:**119–124.
4. **Banyard, A. C., M. D. Baron, and T. Barrett.** 2005. A role for virus promoters in determining the pathogenesis of rinderpest virus in cattle. J Gen. Virol. **86:**1083–1092.
5. **Baron, M. D., A. C. Banyard, S. Parida, and T. Barrett.** 2005. The Plowright vaccine strain of rinderpest virus has attenuating mutations in most genes. J Gen. Virol. **86:**1093–1101.
6. **Baron, M. D., and T. Barrett.** 1997. Rescue of rinderpest virus from cloned cDNA. J. Virol. **71:**1265–1271.
7. **Baron, M. D., Y. Kamata, V. Barras, L. Goatley, and T. Barrett.** 1996. The genome sequence of the virulent Kabete 'O' strain of rinderpest virus: comparison with the derived vaccine. J. Gen. Virol. **77:**3041–3046.
8. **Barrett, T., and P. B. Rossiter.** 1999. Rinderpest: the disease and its impact on humans and animals. Adv. Virus Res. **53:**89–110.
9. **Biacchesi, S., M. H. Skiadopoulos, K. C. Tran, B. R. Murphy, P. L. Collins, and U. J. Buchholz.** 2004. Recovery of human metapneumovirus from cDNA: optimization of growth in vitro and expression of additional genes. Virology **321:**247–259.
10. **Brown, D. D.** 2004. Cross-species infectivity in morbilliviruses. Ph.D. thesis. The Queen's University of Belfast, Northern Ireland, United Kingdom.
11. **Castaneda, S. J., and T. C. Wong.** 1990. Leader sequence distinguishes between translatable and encapsidated measles virus RNAs. J. Virol. **64:**222–230.
12. **Collins, P. L., S. S. Whitehead, A. Bukreyev, R. Fearns, M. N. Teng, K. Juhasz, R. M. Chanock, and B. R. Murphy.** 1999. Rational design of live-attenuated recombinant vaccine virus for human respiratory syncytial virus by reverse genetics. Adv. Virus Res. **54:**423–451.
13. **Crowe, J. E., Jr., P. T. Bui, W. T. London, A. R. Davis, P. P. Hung, R. M. Chanock, and B. R. Murphy.** 1994. Satisfactorily attenuated and protective mutants derived from a partially attenuated cold-passaged respiratory syncytial virus mutant by introduction of additional attenuating mutations during chemical mutagenesis. Vaccine **12:**691–699.
14. **Duprex, W. P., F. M. Collins, and B. K. Rima.** 2002. Modulating the function of the measles virus RNA-dependent RNA polymerase by insertion of green fluorescent protein into the open reading frame. J. Virol. **76:**7322–7328.
15. **Duprex, W. P., I. Duffy, S. McQuaid, L. Hamill, S. L. Cosby, M. A. Billeter, J. Schneider-Schaulies, V. ter Meulen, and B. K. Rima.** 1999. The H gene of rodent brain-adapted measles virus confers neurovirulence to the Edmonston vaccine strain. J. Virol. **73:**6916–6922.
16. **Duprex, W. P., S. McQuaid, L. Hangartner, M. A. Billeter, and B. K. Rima.** 1999. Observation of measles virus cell-to-cell spread in astrocytoma cells by using a green fluorescent protein-expressing recombinant virus. J. Virol. **73:**9568–9575.
17. **Enders, J. F., and T. C. Peebles.** 1954. Propagation in tissue cultures of cytopathic agents from patients with measles. Proc. Soc. Exp. Biol. Med. **86:**277–286.
18. **Evermann, J. F., C. W. Leathers, J. R. Gorham, A. J. McKeirnan, and M. J. Appel.** 2001. Pathogenesis of two strains of lion (*Panthera leo*) morbillivirus in ferrets (*Mustela putorius furo*). Vet. Pathol. **38:**311–316.
19. **Flanagan, E. B., J. M. Zamparo, L. A. Ball, L. L. Rodriguez, and G. W. Wertz.** 2001. Rearrangement of the genes of vesicular stomatitis virus eliminates clinical disease in the natural host: new strategy for vaccine development. J. Virol. **75:**6107–6114.
20. **Forsyth, M. A., and T. Barrett.** 1995. Evaluation of polymerase chain reaction for the detection and characterisation of rinderpest and peste des petits ruminants viruses for epidemiological studies. Virus Res. **39:**151–163.

21. **Friedewald, W. T., B. R. Forsyth, C. B. Smith, M. A. Gharpure, and R. M. Chanock.** 1968. Low-temperature-grown RS virus in adult volunteers. JAMA **203:**690–694.
22. **Griffin, D. E.** 2001. Measles virus, p. 1401–1441. *In* D. M. Knipe, P. M. Howley, D. E. Griffin, R. A. Lamb, M. A. Martin, B. Roizman, and S. E. Straus (ed.), Fields virology, 4th ed. Lippincott Williams & Wilkins, Philadelphia, Pa.
23. **Heaney, J., T. Barrett, and S. L. Cosby.** 2002. Inhibition of in vitro leukocyte proliferation by morbilliviruses. J. Virol. **76:**3579–3584.
24. **Juhasz, K., S. S. Whitehead, C. A. Boulanger, C. Y. Firestone, P. L. Collins, and B. R. Murphy.** 1999. The two amino acid substitutions in the L protein of cpts530/1009, a live-attenuated respiratory syncytial virus candidate vaccine, are independent temperature-sensitive and attenuation mutations. Vaccine **17:**1416–1424.
25. **Katz, S. L., Milovanovic, M. V., and J. F. Enders.** 1958. Propagation of measles virus in cultures of chick embryo cells. Proc. Soc Exp. Biol Med. **97:**23.
26. **Kobune, F., H. Sakata, and A. Sugiura.** 1990. Marmoset lymphoblastoid cells as a sensitive host for isolation of measles virus. J. Virol. **64:**700–705.
27. **Martinez, I., L. L. Rodriguez, C. Jimenez, S. J. Pauszek, and G. W. Wertz.** 2003. Vesicular stomatitis virus glycoprotein is a determinant of pathogenesis in swine, a natural host. J. Virol. **77:**8039–8047.
28. **McIlhatton, M. A., M. D. Curran, and B. K. Rima.** 1997. Nucleotide sequence analysis of the large (L) genes of phocine distemper virus and canine distemper virus (corrected sequence). J. Gen. Virol. **78:**571–576.
29. **Mrkic, B., B. Odermatt, M. A. Klein, M. A. Billeter, J. Pavlovic, and R. Cattaneo.** 2000. Lymphatic dissemination and comparative pathology of recombinant measles viruses in genetically modified mice. J. Virol. **74:**1364–1372.
30. **Mrkic, B., J. Pavlovic, T. Rulicke, P. Volpe, C. J. Buchholz, D. Hourcade, J. P. Atkinson, A. Aguzzi, and R. Cattaneo.** 1998. Measles virus spread and pathogenesis in genetically modified mice. J. Virol. **72:**7420–7427.
31. **Newman, J. T., J. M. Riggs, S. R. Surman, J. M. McAuliffe, T. A. Mulaikal, P. L. Collins, B. R. Murphy, and M. H. Skiadopoulos.** 2004. Generation of recombinant human parainfluenza virus type 1 vaccine candidates by importation of temperature-sensitive and attenuating mutations from heterologous paramyxoviruses. J. Virol. **78:**2017–2028.
32. **Ngichabe, C. K., H. M. Wamwayi, E. K. Ndungu, P. K. Mirangi, C. J. Bostock, D. N. Black, and T. Barrett.** 2002. Long term immunity in African cattle vaccinated with a recombinant capripox-rinderpest virus vaccine. Epidemiol. Infect. **128:**343–349.
33. **Niewiesk, S., I. Eisenhuth, A. Fooks, J. C. Clegg, J. J. Schnorr, S. Schneider-Schaulies, and V. ter Meulen.** 1997. Measles virus-induced immune suppression in the cotton rat (*Sigmodon hispidus*) model depends on viral glycoproteins. J. Virol. **71:**7214–7219.
34. **Nolan, S. M., S. R. Surman, E. Amaro-Carambot, P. L. Collins, B. R. Murphy, and M. H. Skiadopoulos.** 2005. Live-attenuated intranasal parainfluenza virus type 2 vaccine candidates developed by reverse genetics containing L polymerase protein mutations imported from heterologous paramyxoviruses. Vaccine **23:**4765–4774.
35. **Novella, I. S., L. A. Ball, and G. W. Wertz.** 2004. Fitness analyses of vesicular stomatitis strains with rearranged genomes reveal replicative disadvantages. J. Virol. **78:**9837–9841.
36. **Oglesbee, M.** 1992. Intranuclear inclusions in paramyxovirus-induced encephalitis: evidence for altered nuclear body differentiation. Acta Neuropathol. **84:**407–415.
37. **Oldstone, M. B., H. Lewicki, D. Thomas, A. Tishon, S. Dales, J. Patterson, M. Manchester, D. Homann, D. Naniche, and A. Holz.** 1999. Measles virus infection in a transgenic model: virus-induced immunosuppression and central nervous system disease. Cell **98:**629–640.
38. **Plowright, W., and R. D. Ferris.** 1962. Studies with rinderpest virus in tissue culture. The use of attenuated culture virus as a vaccine for cattle. Res. Vet. Sci. **3:**172–182.
39. **Plumet, S., W. P. Duprex, and D. Gerlier.** 2005. Dynamics of viral RNA synthesis during measles virus infection. J. Virol. **79:**6900–6908.
40. **Rall, G. F., M. Manchester, L. R. Daniels, E. M. Callahan, A. R. Belman, and M. B. Oldstone.** 1997. A transgenic mouse model for measles virus infection of the brain. Proc. Natl. Acad. Sci. USA **94:**4659–4663.
41. **Reed, L. J., and H. Muench.** 1938. A simple method for estimating fifty percent endpoints. Am. J. Hyg. **27:**493–497.
42. **Schmidt, U., J. Beyer, U. Polster, L. J. Gershwin, and U. J. Buchholz.** 2002. Mucosal immunization with live recombinant bovine respiratory syncytial virus (BRSV) and recombinant BRSV lacking the envelope glycoprotein G protects against challenge with wild-type BRSV. J. Virol. **76:**12355–12359.
43. **Schwartz, M., J. Chen, W. M. Lee, M. Janda, and P. Ahlquist.** 2004. Alternate, virus-induced membrane rearrangements support positive-strand RNA virus genome replication. Proc. Natl. Acad. Sci. USA **101:**11263–11268.
44. **Skiadopoulos, M. H., S. Surman, J. M. Tatem, M. Paschalis, S. L. Wu, S. A. Udem, A. P. Durbin, P. L. Collins, and B. R. Murphy.** 1999. Identification of mutations contributing to the temperature-sensitive, cold-adapted, and attenuation phenotypes of the live-attenuated cold-passage 45 (cp45) human parainfluenza virus 3 candidate vaccine. J. Virol. **73:**1374–1381.
45. **Takeda, M., K. Takeuchi, N. Miyajima, F. Kobune, Y. Ami, N. Nagata, Y. Suzaki, Y. Nagai, and M. Tashiro.** 2000. Recovery of pathogenic measles virus from cloned cDNA. J. Virol. **74:**6643–6647.
46. **Teng, M. N., S. S. Whitehead, and P. L. Collins.** 2001. Contribution of the respiratory syncytial virus G glycoprotein and its secreted and membrane-bound forms to virus replication in vitro and in vivo. Virology **289:**283–296.
47. **van Binnendijk, R. S., R. W. van der Heijden, G. van Amerongen, F. G. Uytdehaag, and A. D. Osterhaus.** 1994. Viral replication and development of specific immunity in macaques after infection with different measles virus strains. J. Infect. Dis. **170:**443–448.
48. **von Messling, V., D. Milosevic, and R. Cattaneo.** 2004. Tropism illuminated: lymphocyte-based pathways blazed by lethal morbillivirus through the host immune system. Proc. Natl. Acad. Sci. USA **101:**14216–14421.
49. **von Messling, V., C. Springfeld, P. Devaux, and R. Cattaneo.** 2003. A ferret model of canine distemper virus virulence and immunosuppression. J. Virol. **77:**12579–12591.
50. **Walsh, E. P., M. D. Baron, L. F. Rennie, P. Monaghan, J. Anderson, and T. Barrett.** 2000. Recombinant rinderpest vaccines expressing membrane-anchored proteins as genetic markers: evidence of exclusion of marker protein from the virus envelope. J. Virol. **74:**10165–10175.
51. **Whitehead, S. S., C. Y. Firestone, P. L. Collins, and B. R. Murphy.** 1998. A single nucleotide substitution in the transcription start signal of the M2 gene of respiratory syncytial virus vaccine candidate cpts248/404 is the major determinant of the temperature-sensitive and attenuation phenotypes. Virology **247:**232–239.
52. **Wohlsein, P., H. M. Wamwayi, G. Trautwein, J. Pohlenz, B. Liess, and T. Barrett.** 1995. Pathomorphological and immunohistological findings in cattle experimentally infected with rinderpest virus isolates of different pathogenicity. Vet. Microbiol. **44:**141–149.